CrossMark

Overexpression of *MpCYS2*, a phytocystatin gene from *Malus prunifolia* (Willd.) Borkh., confers drought tolerance and protects against oxidative stress in *Arabidopsis*

Yanxiao Tan[1] · Mingjun Li[1] · Fengwang Ma[1]

Abstract Cystatins, or phytocystatins, are plant-specific inhibitors of cysteine proteinases that help regulate endogenous processes and protect plants against heat, salinity, cold, water deficits, chilling, and abscisic acid treatment. *MpCYS2*, a cystatin gene from *Malus prunifolia*, localized to the nucleus, cytoplasm, and plasma membrane in onion epidermal cells. Controlled by the 35S promoter, its ectopic expression in transgenic *Arabidopsis* lines caused accelerated seed germination and greater seedling growth when plants were exposed to osmotic or oxidative stress. Expression by this gene was also associated with enhanced drought tolerance in those transgenics. This positive response was manifested by changes measured in electrolyte leakage, the chlorophyll concentration, and malondialdehyde accumulations. Production of reactive oxygen species (ROS) was appreciably decreased in the dehydration-treated transgenic lines. This gene also influenced root hair development under osmotic-stress conditions. Our findings indicate that *MpCYS2* affects the growth and tolerance of drought-stressed *Arabidopsis* plants possibly because of its influence on ROS accumulations and root hair formation.

Abbreviations

ABA	Abscisic acid
DAB	Diaminobenzidine
EL	Electrolyte leakage
H_2O_2	Hydrogen peroxide
Km	Kanamycin
MDA	Malondialdehyde
MS	Murashige and Skoog
MV	Methyl viologen
NBT	Nitro blue tetrazolium
O_2^-	Superoxide anion
ORF	Open reading frame
PhyCys	Phytocystatins
qRT-PCR	Quantitative real-time PCR
ROS	Reactive oxygen species

Introduction

Cysteine proteinase inhibitors (cystatins) protect cells from damaging endogenous or external proteolysis and may control the intra- or extracellular breakdown of proteins (Turk and Bode 1991). They are widespread in eukaryotes and have been extensively studied in insects and mammals (Margis et al. 1998). More than 80 plant cystatins, i.e., phytocystatins (PhyCys) have been found in various monocot and dicot species, forming an independent sub-family on the cystatin phylogenetic tree (Margis et al. 1998; Rawlings et al. 2008). The PhysCys have no

✉ Fengwang Ma
fwm64@nwsuaf.edu.cn; fwm64@sina.com

1 State Key Laboratory of Crop Stress Biology for Arid Areas, College of Horticulture, Northwest A&F University, Yangling 712100, Shaanxi, People's Republic of China

disulphide bridges or putative glycosylation sites, and can reversibly inhibit the activity of papain-like cysteine proteinases or C13 legumain peptidases, either competitively or non-competitively (Gaddour et al. 2001; Martínez et al. 2007). As with animal cystatins, they have three motifs that interact with their target enzymes. Those include the reactive site Q × V × G in the central loop region, one or two glycine residues near the N-terminus, and an A/PW motif near the C-terminus. In addition, their α-helix has the N-terminal motif LARFAV that forms the hydrophobic core of cystatin molecules (Stubbs et al. 1990).

Phytocystatins modulate endogenous cysteine proteases during protein turnover (Martínez et al. 2009); seed maturation and germination (Arai et al. 2002; Szewińska et al. 2013); mobilization of storage proteins and programmed cell death (Belenghi et al. 2003); and senescence (Sugawara et al. 2002). They also guard against viruses (Gutierrez-Campos et al. 1999), fungi (Martínez et al. 2003; Popovic et al. 2013), and attacks by mites (Carrillo et al. 2011) and other insects (Haq et al. 2004). Research with phytocystatins has led to improvements in the quality of transformed plants. Because ectopic overexpression of phytocystatins can deter insect feeding (Christou et al. 2006; Kiggundu et al. 2010), such a discovery could ultimately mean that fewer pesticides will be needed for agricultural endeavors (Vorster et al. 2010).

Phytocystatin expression is key to acquiring abiotic stress tolerance (van der Vyver et al. 2003; Zhang et al. 2008; Benchabane et al. 2010; Hwang et al. 2010; Wang et al. 2012; Sun et al. 2014). For example, transformed tobacco plants expressing rice cystatin OC-I are more resistant to the challenges that chilling stress poses to photosynthesis (van der Vyver et al. 2003). Transformed Arabidopsis plants that over-express AtCYSa or AtCYSb are more tolerant to high salt, drought, chilling, and oxidative stresses, and the expression of two stress-related proteins, NADP-ME isozyme and APXb, is also stronger (Zhang et al. 2008). The OC-I-inhibited cysteine proteases control plant growth and stress tolerance by influencing the actions of strigolactones (Quain et al. 2014). Although the biological roles of PhysCys genes in plant development and responses to adverse environments have been partly elucidated in Arabidopsis and other species, the mechanisms by which they function at the molecular level are still largely unknown. Likewise, little information is available about their possible roles in fruit crops such as Malus domestica (apple).

Abiotic stress has a detrimental effect on plant growth and food production throughout the world, and drought has the greatest impact on global agriculture (Hayano-Kanashiro et al. 2009; Wang et al. 2013; Tang et al. 2014). Apple is the fourth most economically important woody plant species after citrus, grape, and banana (Hummer and Janick 2009). Therefore, to protect yields and geographic distribution, plant breeders must have appropriate scientific tools to improve rootstock tolerance to water deficits. This includes being able to characterize the gene(s) that encode cystatins.

We previously identified 26 PhyCys genes from the apple genome (Tan et al. 2014). Transcription patterns were studied in several tissue types and in response to drought, low temperature, heat, abscisic acid (ABA), and oxidative stress. Meanwhile, we cloned five of them from M. prunifolia (respective GenBank Accession Nos. KF477272, KF477273, KF477274, KF477275, and KF477276). However, their functions have not been elucidated in detail. Here, we assessed the biological roles of MpCYS2 (GenBank No. KF477273, original name MdCYS15). Our results provide evidence that its ectopic expression conferred drought tolerance in Arabidopsis primarily because fewer ROS were accumulated during the stress response. We also noted that root hair development was changed in overexpressing transgenic lines. This enabled those plants to adapt to osmotic-stress conditions.

Materials and methods

MpCYS2 isolation and sequence analysis

Total RNAs were extracted from the leaves of Malus prunifolia by the CTAB method (Chang et al. 1993). Residual DNA was removed by treating with RNase-free DNase I (Invitrogen, Carlsbad, CA, USA). Integrity of the RNA was checked via electrophoresis on a 1.2 % agarose gel. The first-strand cDNAs were synthesized with 2 µg of total RNA in a 20 µL volume, using a SYBR Prime Script RT-PCR Kit II (TaKaRa, Shiga, Japan). Gene-specific primers (5′-TCCTGATTTCCAACAAACAATACAA-3′ and 5′-AATTTTAAACATTTTGGATCCGAA-3′) were designed according to the Apple Genome Database (http://www.rosaceae.org/projects/apple_genome) to amplify the entire coding region of MpCYS2, with first-strand cDNA used as templates. Afterward, PCR was performed with Taq DNA polymerase (Promega), applying the manufacturer's recommended reaction conditions. Product was retrieved and purified with a DNA Fragment Purification Kit (TaKaRa), then inserted into the pMD-18T vector (TaKaRa). Afterward, positive clones were sequenced with an ABI 3730 sequencer. Sequences were aligned with the ClustalX program (Thompson et al. 1994).

Subcellular localization analysis

To determine the subcellular localization of MpCYS2, we amplified its coding sequences without the termination

codon, using primers 5′-GCTAG<u>TCTAGA</u>ATGATGAAA GTTCCGAT-3′ and 5′-ATA<u>GAGCTC</u>TTTGGGACCGT GAG-3′. PCR was performed with an initial denaturation step at 95 °C for 10 min; followed by 30 cycles of denaturation at 95 °C for 30 s, annealing at 58 °C for 30 s, and extension at 72 °C for 30 s; then a final extension at 72 °C for 10 min. After the amplified cDNA was recovered and sequenced (Invitrogen, Shanghai, China), it was cut with *Xba*I and *Sac*I, and then cloned into the pBI221-GFP vector (Clontech, Palo Alto, CA, USA) under the control of the CaMV35S promoter. The plasmids were sequenced with the above primers (Invitrogen) to confirm the authenticity of the fusion. For examining transient expression, pBI221-MpCYS2-GFP plasmids were transformed into onion epidermal cells with a biolistic helium gun device (PDS-1000; BioRad, Hercules, CA, USA) as described by Diaz et al. (2005). The blank vector pBI221-GFP was used as the control. Cells were then cultured in MS media (Murashige and Skoog 1962) in the dark at 22 °C for 24 h. Afterward, the fluorescent proteins in the epidermal cells were localized at 488 nm using a confocal laser-scanning microscope (LSM510; Carl Zeiss, Thornwood, NY, USA). The GFP fluorescence, chlorophyll auto fluorescence, and light field views were recorded in separate channels, which were then merged to produce an overlay image.

Gene expression analysis by quantitative real-time PCR and semi-quantitative RT-PCR

Total RNA was extracted according to the CTAB method. Residual DNA was removed by treating with RNase-free DNase I (Invitrogen, Carlsbad, CA, USA). Integrity of the RNA was checked via electrophoresis on a 1.2 % agarose gel. The first-strand cDNAs were synthesized with 2 μg of total RNA in a 20-μL volume, using a SYBR Prime Script RT-PCR Kit II (TaKaRa).

Semi RT-PCR was conducted at 94 °C for 3 min; followed by 25 cycles at 94 °C for 30 s, 59 °C for 30 s, and 72 °C for 30 s; with a final elongation at 72 °C for 5 min. Quantitative real-time PCR (qRT-PCR) was performed on an iQ5.0 instrument (Bio-Rad, USA), using SYBR Green qPCR kits (TaKaRa) according to the manufacturer's instructions. Each reaction was conducted in triplicate with a final volume of 20 μL, which included 10.0 μL of SYBR® Premix Ex Taq (TaKaRa), 1.0 μL of cDNA template, 0.8 μL of each primer (10 pmol L^{-1}), and 7.4 μL of ddH2O. The PCR parameters included an initial 95 °C for 3 min; then 40 cycles of 95 °C for 20 s, 60 °C for 20 s, and 72 °C for 20 s. Fluorescence was measured at the end of each cycle. Melting-curve analysis was done by heating the PCR product from 60 to 95 °C. *Arabidopsis Actin* (*AtActin*) was amplified as the internal control. Primers used for semi RT-PCR and qRT-PCR are listed in Supplementary

Table S1. Expression data for *MpCYS2* were presented as relative units after normalization to the *AtActin* control, using the $2^{-\Delta\Delta C_t}$ method. The experiments were repeated three times to minimize inherent errors, and were performed on three separate RNA extracts from three independent samples. Values for mean expression and standard deviation were calculated from the results of those three independent replicates.

Generation of transgenic *Arabidopsis* plants over-expressing *MpCYS2*

The coding region of *MpCYS2* was amplified using primers 5′-GCTAG<u>TCTAGA</u>ATGATGAAAGTTCCGATT-3′ and 5′-ATA<u>GAGCTC</u>TCATTTGGGACCGTGA-3′. PCR was performed with an initial denaturation step at 95 °C for 10 min; followed by 30 cycles of denaturation at 95 °C for 30 s, annealing at 60 °C for 30 s, and extension at 72 °C for 30 s; then a final extension at 72 °C for 10 min. After the amplified cDNA was recovered and sequenced (Invitrogen, Shanghai, China), it was cut with *Xba*I and *Sac*I and ligated into the *Xba*I and *Sac*I sites of binary vector pBI121 (Clontech, Palo Alto, CA, USA), with replacement of the GUS fragment and under the control of the CaMV35S promoter. The construct was introduced into *Agrobacterium tumefaciens* strain EHA105 by electroporation. *Arabidopsis thaliana* ecotype 'Columbia' (Col-0) was transformed via the floral dip method (Clough and Bent 1998), using *Agrobacterium* that contained the recombinant plasmid. Transgenic seeds (T_1) were harvested and sown on an MS medium supplemented with 50 mg L^{-1} kanamycin (Km) as a selectable marker. Afterward, Km-resistant plants were PCR-confirmed using the primers and procedures mentioned above. After further selecting for transgenic lines at a 3:1 segregation ratio, T_3 homozygous lines were derived, and the level of *MpCYS2* expression in those plants was analyzed by semi RT-PCR and qRT-PCR. *Arabidopsis* plants (both transgenic and the wild type, WT) were grown at 22 °C, 100 μmol photons m^{-2} s^{-1}, 70 % relative humidity, and a 16-h long-day photoperiod.

Seed germination tests

To determine their rate of germination, we surface-sterilized and sowed WT and homozygous T_3 transgenic seeds on agar plates containing a 1/2 MS medium supplemented with 0 mM (control) or 200 mM mannitol, 1.0 μM ABA, or 0.5 μM methyl viologen (MV). The plates were held at 4 °C for 3 days before being transferred to growth chambers. The germination status of the three lines was monitored and scored for 7 days on these media. Seeds were considered germinated when the radicles had emerged

1 mm. In each experiment, approximately 100 seeds per line were sown, and triplicate experiments were carried out using independent seed lots.

Stress tolerance tests

For monitoring the effects of stress on the growth of WT and *MpCYS2*-expressing plants, 4-day-old seedlings previously cultured on a solid 1/2 MS medium were transferred and vertically plated onto a 1/2 MS medium either not supplemented (control) or else supplemented with mannitol (200 mM) or MV (0.5 μM). Three replicates were performed for each experiment. After 7 days of treatment, samples were collected for observations of the root hair phenotype and ROS-staining. Root lengths, fresh weights, and chlorophyll concentrations were measured after 10 days of treatment.

In a separate trial, soil-grown plants (2 weeks old) were subjected to water-deficit conditions by withholding irrigation for 10 days. During the drought-treatment period, morphological changes were monitored and photographed when differences became apparent. Their chlorophyll concentrations, electrolyte leakage (EL), and levels of malondialdehyde (MDA) were determined from samples collected at the final time point. Two representative independent transgenic lines (30 plants each for lines OE-2 and OE-5) were assayed. The experiments were repeated thrice with three replicates in each experiment.

Measurements of EL, MDA, and chlorophyll

Electrolyte leakage was determined from *Arabidopsis* leaves as described by Dionisio-Sese and Tobita (1998), with slight modifications. The collected leaves were cut into strips and incubated in 5 mL of distilled water, then placed in a water bath maintained at a constant 32 °C for 2 h. The initial conductivity (C1) was measured using an electrical conductivity meter (DSS-307, Shanghai, China). The samples were then boiled for 15 min to induce complete leakage, and cooled to room temperature before measuring the final electrical conductivity (C2). Calculations followed the formula EL (%) = 100 × C1/C2. The extent of lipid peroxidation was estimated as the concentration of total 2-thiobarbituric acid reactive substances, and was expressed as equivalents of MDA, as reported by Heath and Packer (1968). Chlorophyll was extracted with 80 % acetone, and the concentration was determined spectrophotometrically according to the method of Li et al. (2012).

Observations of the root hair phenotype

The root hairs of seedlings from the WT and lines OE-2 and OE-5 were observed after being treated for 7 days with either 0 (control) or 200 mM mannitol. Images were captured with a fluorescence stereomicroscope (DP72; Olympus, Tokyo, Japan) at 800× magnification in a region that was 5–7 mm from the root tip. Ten plants were collected per genotype per treatment, and three observations were made for each.

Detection of hydrogen peroxide (H_2O_2) and superoxide ion (O_2^-)

Seven-day-old in vitro grown seedlings located at the surface of a solid 1/2 MS medium were placed on dry filter paper for up to 30 min. Afterward, their accumulations of O_2^- and H_2O_2 were detected by histochemical staining methods that used nitro blue tetrazolium (NBT) and diaminobenzidine (DAB), respectively. For O_2^- detection, the samples were incubated under light for 2 h at ambient temperature in a 1 mg mL^{-1} NBT solution prepared in 10 mM phosphate buffer (pH 7.8), until blue spots appeared (Kim et al. 2011). For localization of H_2O_2, excised leaves or whole plants of *Arabidopsis* were placed in a 1 mg mL^{-1} DAB solution (Sigma, Steinheim, Germany). The samples were then incubated in a growth chamber for 8 h until brown spots were visible. The chlorophyll was cleared with concentrated ethanol and the leaves were kept in 70 % ethanol prior to photographing under the fluorescence stereomicroscope (Kotchoni et al. 2006).

Statistical analysis

The treatments were repeated at least thrice with consistent results. Representative photographs were shown here, and data expressed as means and standard errors calculated using Microsoft Excel. The datas were evaluated via one-way analysis of variance (ANOVA), using the SPSS-11 for Windows statistical software package. Statistical differences were compared by Student's *t* tests at significance levels of *$P < 0.05$, **$P < 0.01$, or ***$P < 0.001$.
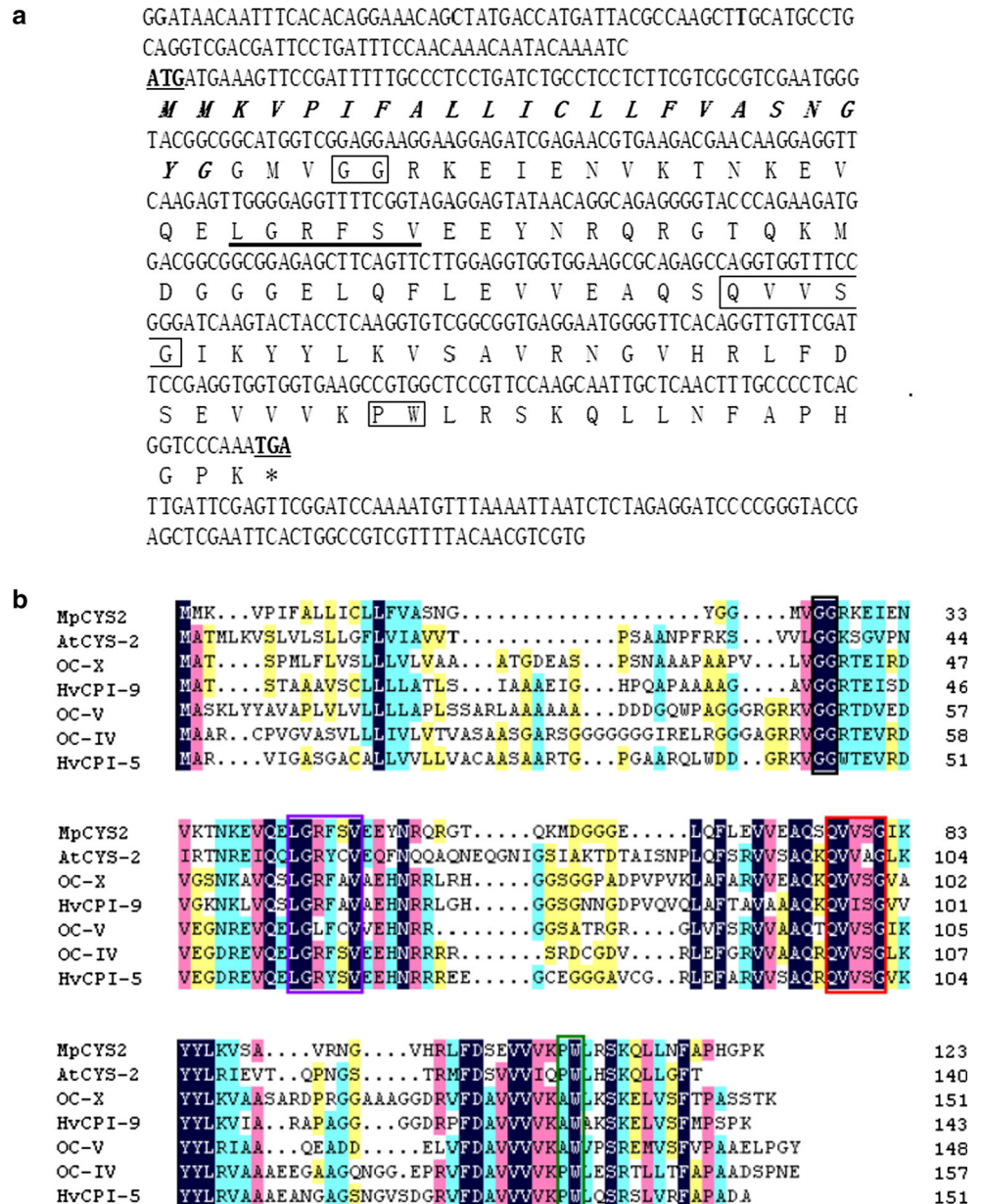
Results

Sequence analysis of *MpCYS2*

We previously isolated the full-length cDNA of *MpCYS2* (GenBank Accession No. KF477273, original name *MdCYS15*) from leaves of *M. prunifolia* (Tan et al. 2014). As shown in Fig. 1a, this cDNA had a 372-bp open reading frame (ORF) plus 3′- and 5′-untranslated regions of 156 and 97 bp, respectively.

Fig. 1 Sequence analysis of *MpCYS2*. **a** Nucleotide and deduced amino acid sequences. *Bold lettering* indicates putative signal peptide. **b** Alignment of deduced amino acid sequence of *MpCYS2* with other members of phytocystatin family: *AtCYS-2* (At2g31980) from *Arabidopsis*; *OC-IV* (Os01g68660), *OC-V* (Os01g68670), and *OC-X* (Os04g2250) from *O. sativa*; and *HvCPI-5* (AJ748340), *HvCPI-9* (AJ748339) from *H. vulgare*. Conserved signature sequences of PhyCys are enclosed with *colored rectangles* (*black*, N-terminal G; *violet*, LARFAV; *red*, QXVXG; *green*, P/AW). (Color figure online)

a

```
GGATAACAATTTCACACAGGAAACAGCTATGACCATGATTACGCCAAGCTTGCATGCCTG
CAGGTCGACGATTCCTGATTTCCAACAAACAATACAAAATC
ATGATGAAAGTTCCGATTTTTGCCCTCCTGATCTGCCTCCTCTTCGTCGCGTCGAATGGG
 M  M  K  V  P  I  F  A  L  L  I  C  L  L  F  V  A  S  N  G
TACGGCGGCATGGTCGGAGGAAGGAAGGAGATCGAGAACGTGAAGACGAACAAGGAGGTT
 Y  G  G  M  V  G G  R  K  E  I  E  N  V  K  T  N  K  E  V
CAAGAGTTGGGGGAGGTTTTCGGTAGAGGAGTATAACAGGCAGAGGGGTACCCAGAAGATG
 Q  E  L  G  R  F  S  V  E  E  Y  N  R  Q  R  G  T  Q  K  M
GACGGCGGCGGAGAGCTTCAGTTCTTGGAGGTGGTGGAAGCGCAGAGCCAGGTGGTTTCC
 D  G  G  G  E  L  Q  F  L  E  V  V  E  A  Q  S  Q V  V  S
GGGATCAAGTACTACCTCAAGGTGTCGGCGGTGAGGAATGGGGTTCACAGGTTGTTCGAT
 G  I  K  Y  Y  L  K  V  S  A  V  R  N  G  V  H  R  L  F  D
TCCGAGGTGGTGGTGAAGCCGTGGCTCCGTTCCAAGCAATTGCTCAACTTTGCCCCTCAC
 S  E  V  V  V  K  P W  L  R  S  K  Q  L  L  N  F  A  P  H
GGTCCCAAATGA
 G  P  K  *
TTGATTCGAGTTCGGATCCAAAATGTTTAAAATTAATCTCTAGAGGATCCCCGGGTACCG
AGCTCGAATTCACTGGCCGTCGTTTTACAACGTCGTG
```

b

To investigate the phylogenetic relationship between apple cystatin genes and previously characterized phytocystatin genes from rice, *Arabidopsis*, and barley, we constructed a phylogenetic dendrogram, and the tree revealed that *MpCYS2* formed a close cluster with *AtCYS-2*, *HvCPI-9*, *OC-X*, *OC-V*, *OC-IV*, and *HvCPI-5*, all of which were distributed in Group B (Tan et al. 2014). Here, amino acid sequences were aligned for *MpCYS2*, *AtCYS-2*, *HvCPI-9*, *OC-X*, *OC-V*, *OC-IV*, and *HvCPI-5* (Fig. 1b). Characteristic sequences and motifs of PhyCys are highlighted, including one or two Glys residues (G/GG) at the N-terminal, the reactive site QXVXG in the central part, and the P/AW residues near the C-terminal. We also

localized the LARFAV sequence, typical of PhyCys, near the N-terminal end of the protein.

Subcellular localization of *MpCYS2*

To investigate the subcellular localization of *MpCYS2*, we cloned its ORF into an expression vector that appended GFP to the C-terminus of the protein. Plasmid pBI221-MpCYS2-GFP was transiently transformed into onion epidermal cells by biolistic bombardment. The GFP alone was used as an internal control. Data obtained through confocal laser-scanning microscopy showed that the fluorescence signals of *MpCYS2*-GFP were similar to GFP

alone, being distributed not only throughout the cytoplasm, but also in the nucleus (Fig. 2).

Constitutive expression of *MpCYS2* in transgenic *Arabidopsis*

We previously demonstrated that *MpCYS2* expression can be induced by water-deficit, MV, or exogenous ABA treatments (Tan et al. 2014). To examine further the potential function of *MpCYS2* in response to drought and oxidative stresses, we transformed its ORF into *Arabidopsis* under the control of a 35S promoter. In all, 37 independent transgenic lines were obtained and verified by PCR analysis (data not shown). Among them, 21 exhibited higher expression, based on semi RT-PCR and qRT-PCR analysis (data not shown). Two representative lines—OE-2 and OE-5—with the highest expression of *MpCYS2* were selected for subsequent examinations (Fig. 3).

Germination of *Arabidopsis* seeds under ABA, osmotic, and oxidative stresses

Because *MpCYS2* was expressed in response to drought, MV-induced oxidative stress, or exogenous ABA treatment, plate germination assays were employed to test the effect this gene had on seed germination under those conditions. In the normal growth scenario, germination for 35S:*MpCYS2* was retarded when compared with the WT (Fig. 4a). On the medium containing mannitol, MV, or ABA, germination of both WT- and transgenics-derived seeds was repressed, but clear differences were noted. After 5 days on the MS medium supplemented with 200 mM mannitol, only 68 % of the WT seed but more than 96 % of the seed from *MpCYS2*-expressing plants had germinated (Fig. 4b). Similarly, when exposed to MS media containing 0.5 μM MV, germination rates were lower for the WT than for the transgenic lines at each time point (Fig. 4c). However, ABA inhibited germination of 35S:*MpCYS2* plants more severely than that of the WT. Treatment with 1.0 μM ABA decreased the rate for 35S:*MpCYS2* plants to

approximately 40 % on Day 4 while WT retained 90 % germination under the same conditions (Fig. 4d).

Overexpression of *MpCYS2* in *Arabidopsis* enhanced tolerance to drought and oxidative stresses

To determine the effects of stress on seedling growth, we placed *Arabidopsis* seeds on a standard 1/2 MS medium for 4 days. Following germination, the seedlings were transferred to media supplemented with mannitol or MV. On the control (unsupplemented) medium, elongation of the primary roots from transgenic seedlings was delayed significantly compared with that of the WT, and fresh weights followed a parallel trend. However, WT growth was severely inhibited upon exposure to excess mannitol for 10 days, leading to a depression in root lengths of approximately 22–28 %, as well as a reduction in fresh weights of about 32–45 % when compared with the transgenic lines (Fig. 5a, b). The WT cotyledons were bleached by the end of the treatment period while those from transgenic plants showed significant resistance to MV-induced damage (Fig. 5a). Chlorophyll loss was significantly delayed in the *MpCYS2*-expressing plants (Fig. 5c). All of these results showed that *MpCYS2* expression alleviated the negative effects imposed by osmotic and oxidative stress on plant growth.

We also performed drought-tolerance experiments with soil-grown plants by withholding water for as long as 10 days. At the onset of this treatment, no obvious difference was observed among the tested lines. However, as the stress period was prolonged, two transgenic lines showed better growth than the WT (Fig. 6a). Measurements confirmed this phenotype, with the transgenics having significantly less electrolyte leakage and higher chlorophyll concentrations (Fig. 6b).

Production of ROS under dehydration treatment

Two major indicators of ROS accumulation that can be induced by many environmental stresses—H_2O_2 and O_2^-—were monitored with DAB and NBT histochemical

Fig. 2 Subcellular localization of *MpCYS2*–GFP fusion protein in onion epidermal cells. GFP fluorescence, bright field, and overlay from merging of bright and fluorescent illumination are shown
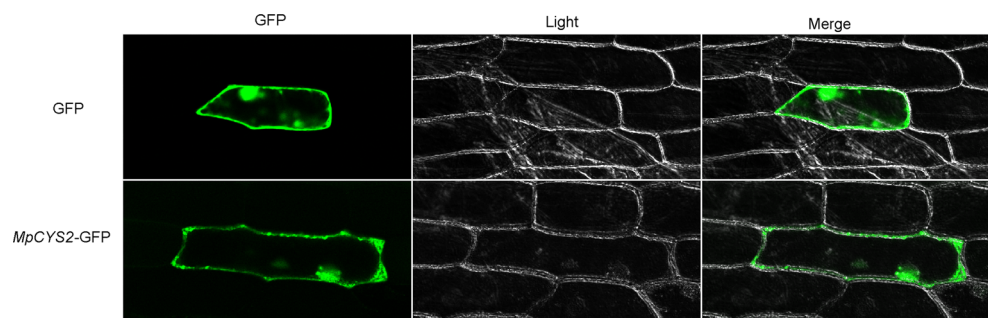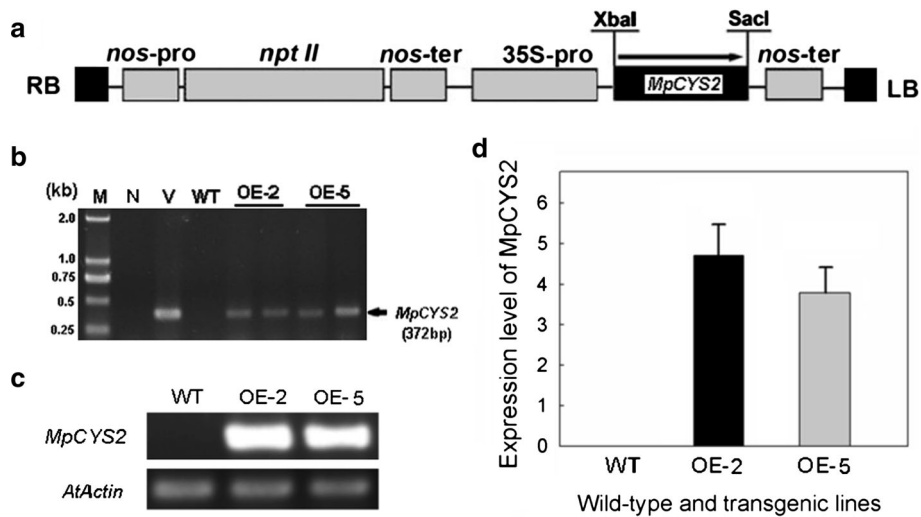
Fig. 3 Molecular characterizations of untransformed WT and transgenic *Arabidopsis thaliana* plants. **a** Structure of 35S:*MpCYS2* construct for expression of *MpCYS2*. Gene encoding bacterial neomycin phosphotransferase II (*npt II*), which is regulated by nopaline synthase gene promoter (*nos*-pro) and 3′-terminator (*nos*-ter), served as selectable marker for *Arabidopsis* transformation. *MpCYS2* was regulated by CaMV 35S promoter (35S-pro). LB and RB indicate *left* and *right* T-DNA borders, respectively. **b** PCR analysis of untransformed WT and transgenic *Arabidopsis* plants.

Presence of *MpCYS2* was verified by PCR amplification using gene-specific primers shown in Supplementary Table S1. *Lanes*: *M*, molecular size marker; *N*, negative control (double-distilled water); *V*, 35S:*MpCYS2* vector; OE-2 and OE-5, two independent 35S:*MpCYS2* lines. **c**, **d** Semi RT-PCR and quantitative real-time PCR analysis of *MpCYS2* mRNA levels in 3-week-old seedling leaves from WT and two independent transgenic lines (OE-2, OE-5) that over-expressed *MpCYS2*. Both experiments in (**c**) and d were repeated three times. *AtActin* served as control
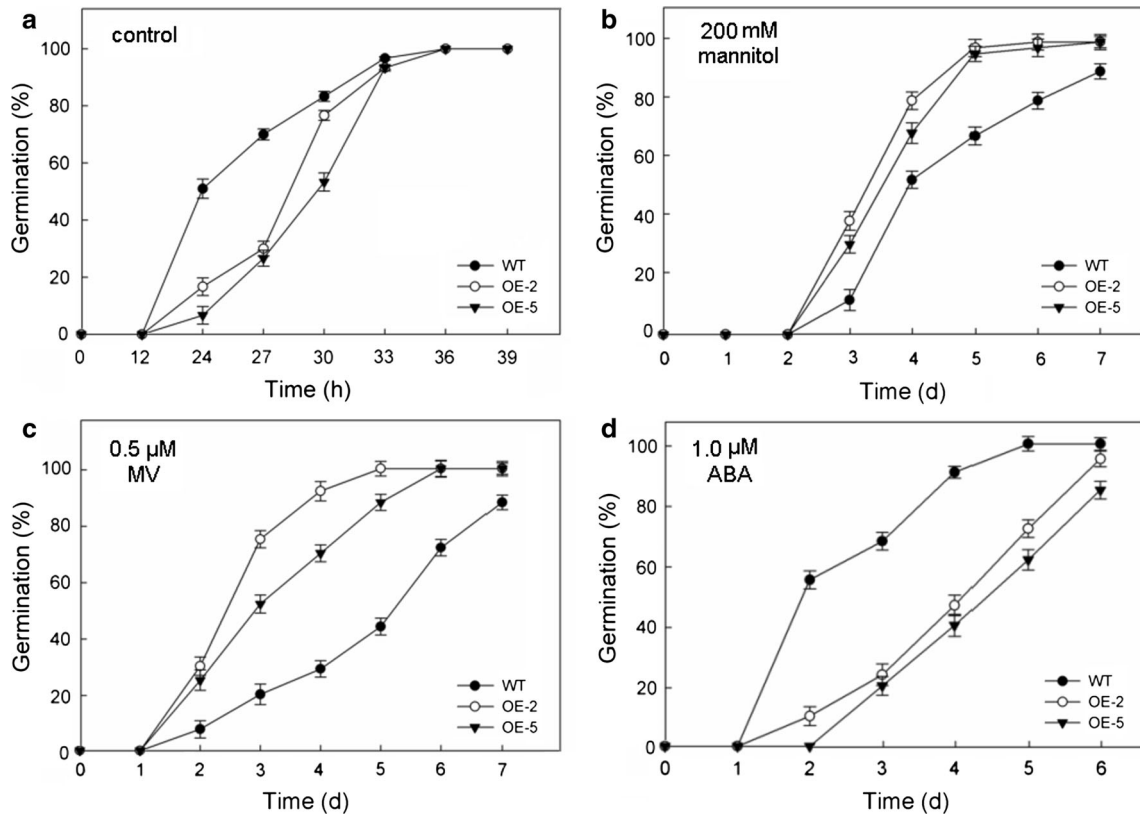
Fig. 4 Germination rates of seeds from WT and transgenic *Arabidopsis* plants (OE-2, OE-5) sown on 1/2 MS media supplemented with 0 mM (control) (**a**), or 200 mM mannitol (**b**), 1.0 μM ABA

(**c**) or 0.5 μM MV (**d**). Results are mean ± SD from three independent experiments (approximately 100 seeds per line were sown for each experiment)
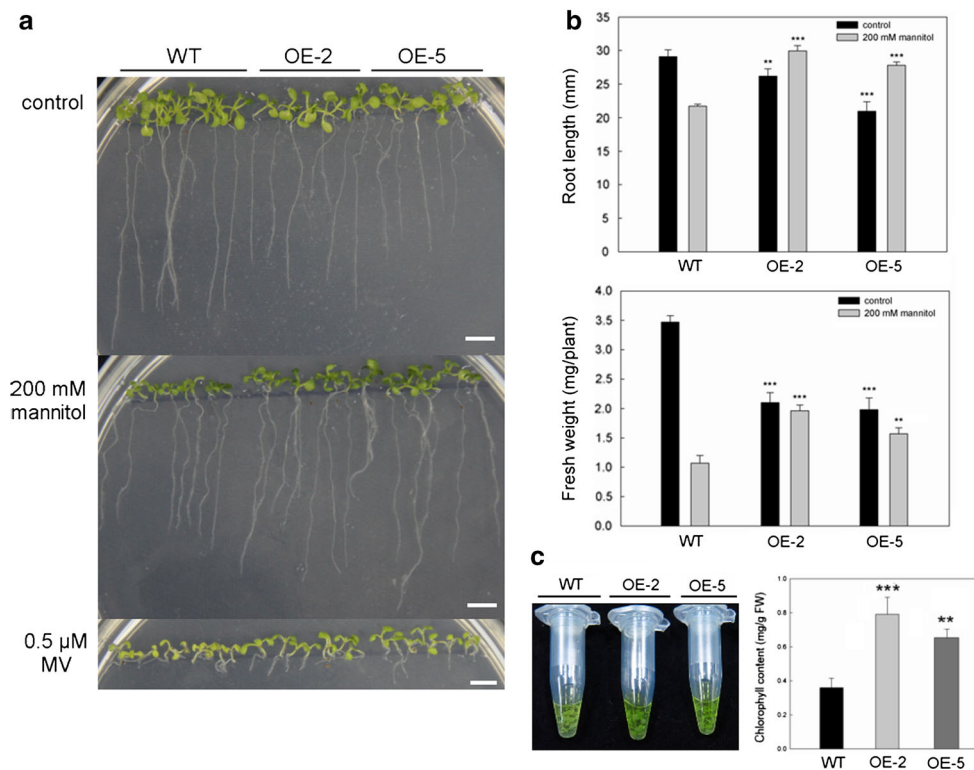
Fig. 5 Effects of osmotic and oxidative stresses on growth of WT and transgenic seedlings (OE-2, OE-5). **a** Representative photograph of phenotypes for WT (control; no supplements) and transgenic seedlings grown for 10 days on 1/2 MS medium supplemented with 200 mM mannitol or 0.5 μM methyl viologen (MV). **b** Root lengths and fresh weights of WT and transgenic seedlings after 10 days of treatment with 200 mM mannitol. **c** Chlorophyll concentration was determined from WT and transgenic seedlings after 10 days of treatment with MV (0.5 μM). Results are means and SDs from three independent experiments (approximately 10 seedlings per line per experiment). Data were significantly different from WT values at **$P < 0.01$ or ***$P < 0.001$, based on Student's t tests. *Scale bar* 5 mm

staining, respectively. Under control conditions, no significant difference was observed among the WT and transgenics (Fig. 7a). After dehydration treatment, however, the in vitro seedlings of the transgenic lines accumulated much less ROS (Fig. 7b). These accumulations can directly react with proteins, amino acids, and nucleic acids, and cause lipid peroxidation, which can then be estimated based on the amount of MDA produced. Here, the levels of MDA found in the leaves of both WT and *MpCYS2*-expressing plants increased substantially following water-deficit treatment, although concentrations were significantly lower in the transgenic lines (Fig. 6b). These results suggested that constitutive expression of *MpCYS2* enhanced tolerance to oxidative stress-induced membrane hydroperoxidation in our transformed *Arabidopsis* plants (lines OE-2 and OE-5).

MpCYS2 affected root hair development in response to osmotic stress

Root hairs have important roles in water and nutrient uptake (Clarkson 1985), anchoring the plant in the soil, and interacting with microorganisms (Bauer 1981). Because we had observed overt morphological differences between the WT and transgenic seedlings when they were treated with 200 mM mannitol for 7 days, we assessed their root hair phenotypes. Under control conditions, 35S:*MpCYS2* seedlings (OE-2, OE-5) showed higher density but shorter length of root hairs in comparison with the WT. When the MS medium was supplemented with 200 mM mannitol, more and longer root hairs developed in the transgenic lines to adapt to osmotic-stress conditions whereas no significant changes appeared in the WT (Fig. 8). Therefore, these results indicated that *MpCYS2* expression affected root hair development under stress conditions, thereby having a positive impact on osmotic stress tolerance.

Discussion

The PhyCys help regulate endogenous processes and guard against the effects of various biotic or abiotic stresses (Gutierrez-Campos et al. 1999; Arai et al. 2002; Haq et al. 2004; Valdés-Rodríguez et al. 2007; Zhang et al. 2008;

Fig. 6 Comparison of drought tolerance between WT and transgenic *Arabidopsis* (30 plants per line per experiment). **a** Phenotypes of 2-week-old soil-grown plants of WT and transgenic lines (OE-2, OE-5) in response to water-deficit treatment for 10 days. **b** Chlorophyll content, electrolyte leakage, and MDA accumulation measured after 10 days. Results are mean ± SD from three independent experiments. Data were significantly different from WT values at *$P < 0.05$ or ***$P < 0.001$, based on Student's *t* tests
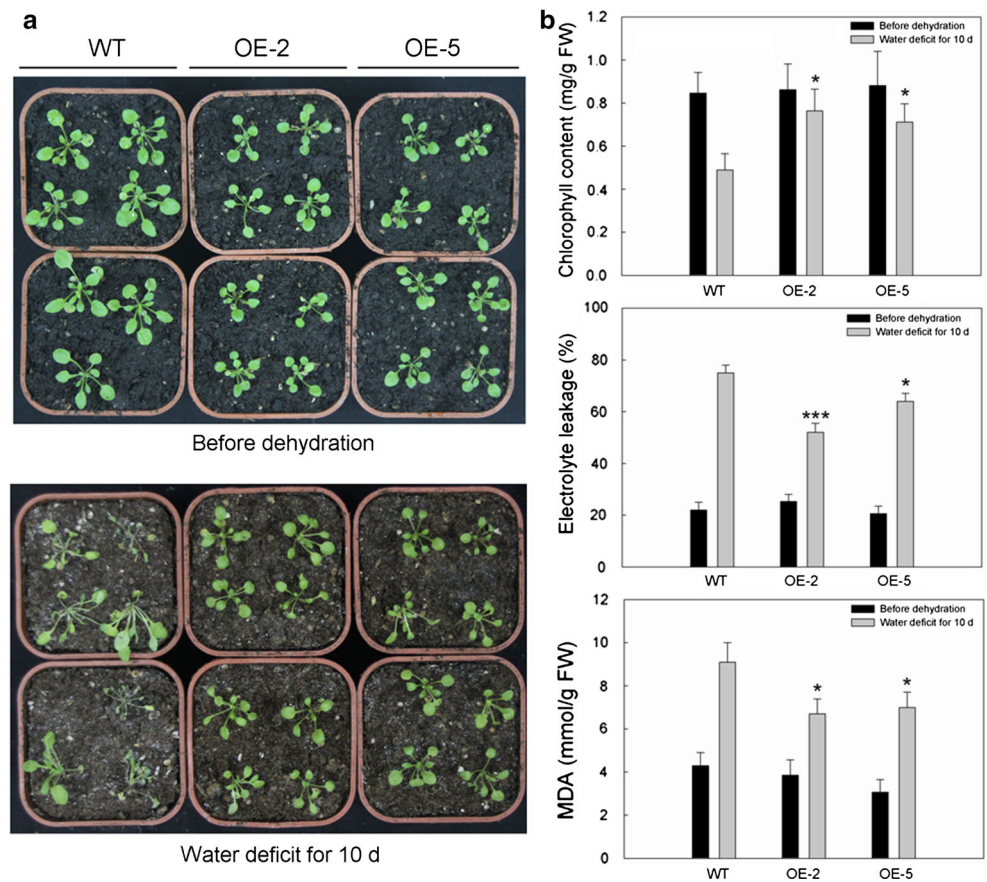
Fig. 7 Histochemical staining assay of ROS accumulation with nitro blue tetrazolium (NBT) and diaminobenzidine (DAB) in WT and transgenic seedlings (OE-2, OE-5) that were either untreated (control) (**a**) or subjected to dehydration for 30 min (**b**)
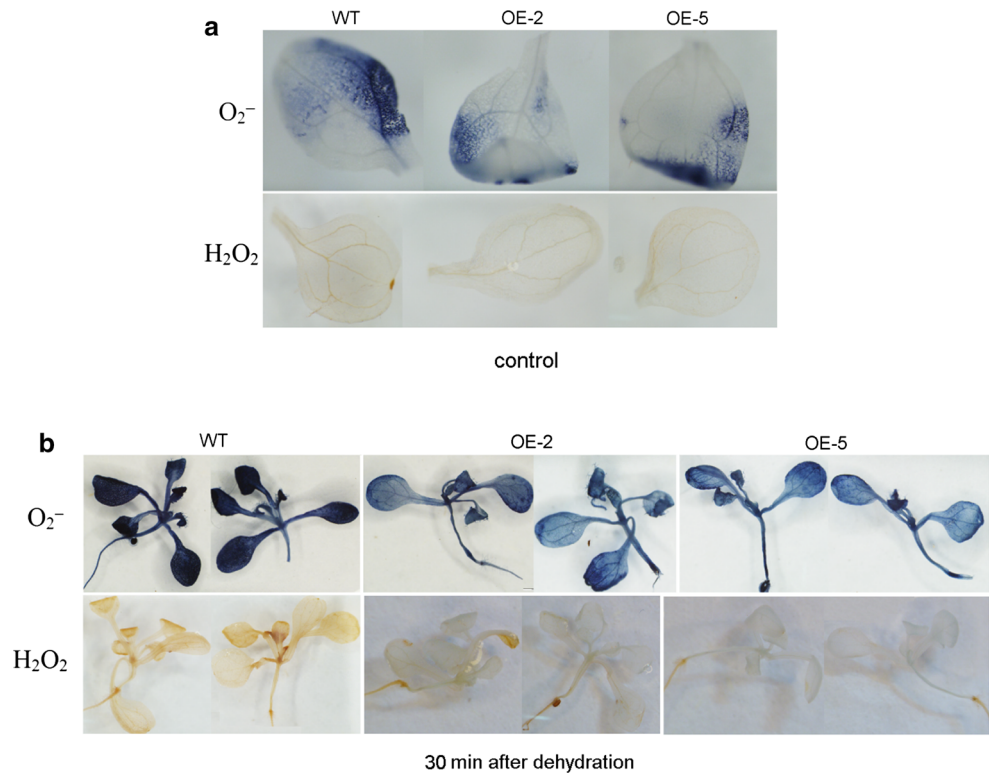
Fig. 8 Root hair phenotypes of WT and transgenic lines (OE-2, OE-5) plants treated with 0 (control) or 200 mM mannitol for 7 days. Representative photographs were captured at ×800 magnification through fluorescence stereomicroscope in region of 5–7 mm from root tip
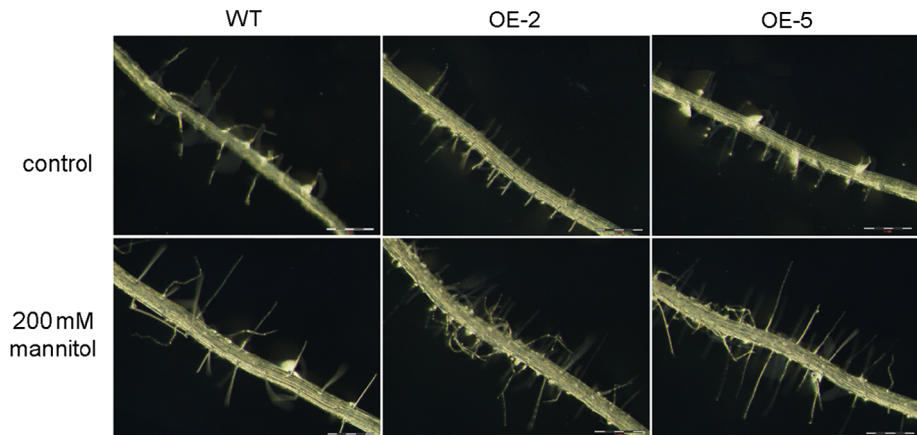
Hwang et al. 2010). We previously identified cystatin genes within the entire apple genome and monitored their transcription patterns in several tissues and in response to drought, low temperature, heat, ABA, and oxidative stress (Tan et al. 2014). However, their biological functions had not yet been systematically evaluated. Here, we detail the roles of *MpCYS2*, a cystatin gene from *M. prunifolia*.

MpCYS2 contains one cystatin-like domain and functional motifs that are common to other phytocystatins (Kimura et al. 1995; Lim et al. 1996). Phylogenetic analysis clearly demonstrated that this gene is closely related to *AtCYS-2*, *HvCPI-9*, *OC-X*, *OC-V*, *OC-IV*, and *HvCPI-5* within Cluster B of the four cystatin clusters (Tan et al. 2014). Furthermore, we found that the fluorescence signals of *MpCYS2*-GFP fusion protein were similar to GFP alone, which distributed uniformly throughout the entire cellular space, including the nucleus, cytoplasm, and plasma membrane. This was consistent with reports for other cystatin genes, such as *BvM14-cystatin* from *Beta vulgaris* (sugar beet) 'M14' (Wang et al. 2012) and *GsCPI14* from *Glycine soja* (Sun et al. 2014).

The mRNA accumulation of *MpCYS2* was induced by drought, oxidation, or ABA treatment (Tan et al. 2014). These results implied that this stress–responsive gene is involved in different signaling pathways that are triggered in apple by abiotic stresses. Subsequently, we introduced *MpCYS2* into model plant *Arabidopsis*, which led to undesirable side effects such as retarded seed germination, decreased seedling growth, and diminished root development under normal conditions. These observations concurred with those of Hwang et al. (2009). It is possible that *MpCYS2* might inhibit the activity of some endogenous cysteine proteinases, which are responsible for the degradation of seed storage proteins during seed germination and early seedling growth. By contrast, tolerance was enhanced when plants were exposed to abiotic stresses. For example, seeds of *Arabidopsis* from the 35S:*MpCYS2* transgenic lines (lines OE-2 and OE-5) germinated earlier than those

of the WT when the medium was supplemented with mannitol or MV. However, 35S:*MpCYS2* was hypersensitive to ABA during germination. We speculated that *MpCYS2* might play different roles in different stress pathways, thereby leading to various degrees of sensitivity to different stresses. Furthermore, seedlings of the two overexpressing lines (OE-2 and OE-5) showed improved root growth and had higher fresh weights under osmotic stress conditions. Soil-grown mature plants from those lines also performed better and experienced less severe oxidative stress under a water deficit. Those outcomes were easily manifested by changes in the values calculated for physiological parameters, including cell membrane damage (via EL data), chlorophyll concentration, and the extent of lipid peroxidation (i.e., levels of MDA). This was further evidence that the enhancement of stress tolerance persists throughout the vegetative growth period.

In plants, extreme environments often lead to oxidative stress due to the generation of ROS, including H_2O_2, O_2^-, and the hydroxyl radical ·OH, all of which cause cellular damage and death (Mittler 2002; Ramanjulu and Bartels 2002). This ROS response is thought to be a major reason for those adverse effects. Here, less ROS was accumulated and visualized via staining in transgenic seedlings than in the WT upon dehydration treatment. These findings suggested a possible mode for the action of *MpCYS2* under drought stress, with this gene at least partially modulating ROS homeostasis. It was also observed by Zhang et al. (2008) that *APXb* accumulated a little abundantly in some of *AtCYSa* and *AtCYSb* transgenic plants compared with that of in WT plants under salt stress condition, which could be activated by different types of stress and played important role in ROS-scavenging (Apel and Hirt 2004; Davletova et al. 2005).

As a major environmental stress, drought imposes adverse effects on plant growth and development (Denby and Gehring 2005; Liu et al. 2015). Nevertheless, plants utilize several mechanisms for coping at the morphological,

anatomical, and cellular levels (Bray 1997). Examples include increased production of lateral roots (Jupp and Newman 1987) or the stimulation of root hair density and proliferation, which can increase the total root surface area and improve plant water uptake in arid regions (White and Kirkegaard 2010). Root hairs are single-walled cells where many water channels and phosphate, nitrogen, potassium, calcium, and sulfate transporters are localized, all of which are beneficial to water and nutrient uptake (Libault et al. 2010). Root hair development may help facilitate water uptake and root survival in drying soils. Our results indicated that *MpCYS2* expression influences the length and destiny of root hairs in response to osmotic stress, which ultimately has a positive effect on stress tolerance. Its involvement in determining root hair growth under such conditions leads us to propose that *MpCYS2* in *Arabidopsis* has a regulatory role in the abiotic stress response.

Taken together, our research data provide novel information that increases our understanding about the roles of *MpCYS2* in response to environmental stresses. The phenotypic comparisons between overexpressing transgenic plants and the WT imply that *MpCYS2* acts as a positive regulator of seed germination as well as plant growth and development in adverse environments. Moreover, this gene is apparently involved in controlling ROS accumulations in drought-stressed plants. We have also identified a new function for *MpCYS2* in conferring abiotic stress tolerance, based on how its expression influences root hair development for adaptations to osmotic stress conditions. Nevertheless, such observations of the pleiotropic effects by this recombinant protease inhibitor in planta show that our current knowledge of the range of functions for plant proteolytic processes is incomplete. Thus, cysteine protease inhibitors might also be an attractive target that will allow researchers to improve the traits of stress tolerance in transformed plants. Further investigations should focus on elucidating the cellular mechanisms that support *MpCYS2*-mediated drought stress tolerance in apple.

Compliance with Ethical Standards

Conflict of interest The authors declare no competing financial interests.

References

Apel K, Hirt H (2004) Reactive oxygen species: metabolism, oxidative stress, and signal transduction. Annu Rev Plant Biol 55:373–399

Arai S, Matsumoto I, Emori Y, Abe K (2002) Plant seed cystatins and their target enzymes of endogenous and exogenous origin. J Agric Food Chem 50:6612–6617

Bauer WD (1981) Infection of legumes by rhizobia. Annu Rev Plant Physiol 32:407–449

Belenghi B, Acconcia F, Trovato M, Perazzolli M, Bocedi A, Polticelli F, Ascenzi P, Delledonne M (2003) *AtCYS1*, a cystatin from *Arabidopsis thaliana*, suppresses hypersensitive cell death. Eur J Biochem 270:2593–2604

Benchabane M, Schlüter U, Vorster J, Goulet MC, Michaud D (2010) Plant cystatins. Biochimie 92:1657–1666

Bray EA (1997) Plant responses to water deficit. Trends Plant Sci 2:48–54

Carrillo L, Martínez M, Ramessar K, Cambra I, Castañera P, Ortego F, Díaz I (2011) Expression of a barley cystatin gene in maize enhances resistance against phytophagous mites by altering their cysteine-proteases. Plant Cell Rep 30:101–112

Chang S, Puryear J, Cairney J (1993) A simple and efficient method for isolating RNA from pine trees. Plant Mol Biol Report 11:113–116

Christou P, Capell T, Kohli A, Gatehouse J, Gatehouse A (2006) Recent developments and future prospects in insect pest control in transformed crops. Trends Plant Sci 11:302–308

Clarkson D (1985) Factors affecting mineral nutrient acquisition by plants. Annu Rev Plant Physiol 36:77–115

Clough SJ, Bent AF (1998) Floral dip: a simplified method for *Agrobacterium*-mediated transformation of *Arabidopsis thaliana*. Plant J 16:735–743

Davletova S, Rizhsky L, Liang H, Shengqiang Z, Oliver DJ, Coutu J, Shulaev V, Schlauch K, Mittler R (2005) Cytosolic ascorbate peroxidase 1 is a central component of the reactive oxygen gene network of *Arabidopsis*. Plant Cell 17:268–281

Denby K, Gehring C (2005) Engineering drought and salinity tolerance in plants: lessons from genome-wide expression profiling in *Arabidopsis*. Trends Biotechnol 23:547–552

Diaz I, Martinez M, Isabel-LaMoneda I, Rubio-Somoza I, Carbonero P (2005) The DOF protein, SAD, interacts with GAMYB in plant nuclei and activates transcription of endosperm-specific genes during barley seed development. Plant J 42:652–662

Dionisio-Sese ML, Tobita S (1998) Antioxidant responses of rice seedlings to salinity stress. Plant Sci 135:1–9

Gaddour K, Vicente-Carbajosa J, Lara P, Isabel-Lamoneda I, Díaz I, Carbonero P (2001) A constitutive cystatin-encoding gene from barley (*Icy*) responds differentially to abiotic stimuli. Plant Mol Biol 45:599–608

Gutierrez-Campos R, Torres-Acosta JA, Saucedo-Arias LJ, Gomez-Lim MA (1999) The use of cysteine proteinase inhibitors to engineer resistance against potyviruses in transgenic tobacco plants. Nat Biotechnol 17:1223–1226

Haq SK, Atif SM, Khan RH (2004) Protein proteinase inhibitor genes in combat against insects, pests, and pathogens: natural and engineered phytoprotection. Arch Biochem Biophys 431:145–159

Hayano-Kanashiro C, Calderon-Vazquez C, Ibarra-Laclette E, Herrera-Estrella L, Simpson J (2009) Analysis of gene expression and physiological responses in three Mexican maize landraces under drought stress and recovery irrigation. PLoS One 4:e7531

Heath RL, Packer L (1968) Photoperoxidation in isolated chloroplasts: I. Kinetics and stoichiometry of fatty acid peroxidation. Arch Biochem Biophys 125:189–198

Hummer KE, Janick J (2009) Rosaceae: taxonomy, economic importance, genomics. In: Folta K, Gardiner S (eds) Genetics and genomics of Rosaceae. Springer, New York, pp 1–17

Hwang JE, Hong JK, Je JH, Lee KO, Kim DY, Lee SY, Lim CO (2009) Regulation of seed germination and seedling growth by

an *Arabidopsis* phytocystatin isoform, *AtCYS6*. Plant Cell Rep 28:1623–1632

Hwang JE, Hong JK, Lim CJ, Chen H, Je J, Yang KA, Kim DY, Choi YJ, Lee SY, Lim CO (2010) Distinct expression patterns of two *Arabidopsis* phytocystatin genes, *AtCYS1* and *AtCYS2*, during development and abiotic stresses. Plant Cell Rep 29:905–915

Jupp AP, Newman EI (1987) Morphological and anatomical effects of severe drought on the roots of *Lolium perenne* L. New Phytol 105:393–402

Kiggundu A, Muchwezi J, van der Vyver C, Viljoen A, Vorster J, Schlüter U, Kunert K, Michaud D (2010) Deleterious effects of plant cystatins against the banana weevil *Cosmopolites sordidus*. Arch Insect Biochem Physiol 73:87–105

Kim SH, Woo DH, Kim JM, Lee SY, Chung WS, Moon YH (2011) *Arabidopsis* MKK4 mediates osmotic-stress response via its regulation of MPK3 activity. Biochem Biophys Res Commun 412:150–154

Kimura M, Ikeda T, Fukumoto D, Yamasaki N, Yonekura M (1995) Primary structure of a cysteine proteinase inhibitor from the fruit of avocado (*Persea americana* Mill). Biosci Biotechnol Biochem 59:2328–2329

Kotchoni SO, Kuhns C, Ditzer A, Kirch H-H, Bartels D (2006) Over-expression of different aldehyde dehydrogenase genes in *Arabidopsis thaliana* confers tolerance to abiotic stress and protects plants against lipid peroxidation and oxidative stress. Plant Cell Environ 29:1033–1048

Li D, Song S, Xia X, Yin W (2012) Two CBL genes from populus euphratica confer multiple stress tolerance in transgenic triploid white poplar. Plant Cell Tissue Organ Cult 109:477–489

Libault M, Brechenmacher L, Cheng JL, Xu D, Stacey G (2010) Root hair systems biology. Trends Plant Sci 15:641–650

Lim CO, Lee SI, Chung WS, Park SH, Hwang I, Cho MJ (1996) Characterization of a cDNA encoding a cysteine proteinase inhibitor from Chinese cabbage (*Brassica campestris* L. ssp. *pekinensis*) flower buds. Plant Mol Biol 30:373–379

Liu YB, Qin LJ, Han LZ, Xiang Y, Zhao DG (2015) Overexpression of maize *SDD1* (*ZmSDD1*) improves drought resistance in *Zea mays* L. by reducing stomatal density. Plant Cell Tissue Organ Cult 122:147–159

Margis R, Reis EM, Villeret V (1998) Structural and phylogenetic relationships among plant and animal cystatins. Arch Biochem Biophys 359:24–30

Martínez M, López-Solanilla E, Rodríguez-Palenzuela P, Carbonero P, Díaz I (2003) Inhibition of plant-pathogenic fungi by the barley cystatin Hv-CPI (gene *Icy*) is not associated with its cysteine-proteinase inhibitory properties. Mol Plant Microbe Interact 16:876–883

Martínez M, Diaz-Mendoza M, Carrillo L, Díaz I (2007) Carboxy terminal extended phytocystatins are bifunctional inhibitors of papain and legumain cysteine proteinases. FEBS Lett 581:2914–2918

Martínez M, Cambra I, Carrillo L, Diaz-Mendoza M, Diaz I (2009) Characterization of the entire cystatin gene family in barley and their target cathepsin L-like cysteine-proteases, partners in the hordein mobilization during seed germination. Plant Physiol 151:1531–1545

Mittler R (2002) Oxidative stress, antioxidants and stress tolerance. Trends Plant Sci 7:405–410

Murashige T, Skoog F (1962) A revised medium for rapid growth and bioassay with tobacco tissue cultures. Physiol Plant 15:473–497

Popovic M, Andjelkovic U, Burazer L, Lindner B, Petersen A, Gavrovic-Jankulovic M (2013) Biochemical and immunological characterization of a recombinantly-produced antifungal cysteine proteinase inhibitor from green kiwifruit (*Actinidia deliciosa*). Phytochemistry 94:53–59

Quain MD, Makgopa ME, Márquez-García B, Comadira G, Fernandez-Garcia N, Olmos E, Schnaubelt D, Kunert KJ, Foyer CH (2014) Ectopic phytocystatin expression leads to enhanced drought stress tolerance in soybean (*Glycine max*) and *Arabidopsis thaliana* through effects on strigolactone pathways and can also result in improved seed traits. Plant Biotechnol J 12:903–913

Ramanjulu S, Bartels D (2002) Drought- and desiccation-induced modulation of gene expression in plants. Plant Cell Environ 25:141–151

Rawlings ND, Morton FR, Barrett AJ (2008) MEROPS: the peptidase database. Nucl Acids Res 36:320–325

Stubbs MT, Laber B, Bode W, Huber R, Jerala R, Lenarcic B, Turk V (1990) The refined 2.4 Å X-ray crystal structure of recombinant human stefin B in complex with the cysteine proteinase papain: a novel type of proteinase inhibitor interaction. EMBO J 9:1939–1947

Sugawara H, Shibuya K, Yoshioka T, Hashiba T, Satoh S (2002) Is a cysteine proteinase inhibitor involved in the regulation of petal wilting in senescing carnation (*Dianthus caryophyllus* L.) flowers? J Exp Bot 53:407–413

Sun XL, Yang SS, Sun MZ, Wang ST, Ding XD, Zhu D, Ji W, Cai H, Zhao CY, Wang XD, Zhu YM (2014) A novel Glycine soja cysteine proteinase inhibitor GsCPI14, interacting with the calcium/calmodulin-binding receptor-like kinase GsCBRLK, regulated plant tolerance to alkali stress. Plant Mol Biol 85:33–48

Szewińska J, Prabucka B, Krawczyk M, Mielecki M, Bielawski W (2013) The participation of phytocystatin *TrcC-4* in the activity regulation of *EP8*, the main prolamin degrading cysteine endopeptidase in triticale seeds. Plant Growth Regul 69:131–137

Tan YX, Wang SC, Liang D, Li MJ, Ma FW (2014) Genome-wide identification and expression profiling of the cystatin gene family in apple (*Malus × domestica* Borkh.). Plant Physiol Biochem 79:88–97

Tang LL, Cai H, Zhai H, Luo X, Wang ZY, Cui L, Bai X (2014) Overexpression of *Glycine soja WRKY20* enhances both drought and salt tolerance in transgenic alfalfa (*Medicago sativa* L.). Plant Cell Tissue Organ Cult 118:77–86

Thompson JD, Higgins DG, Gibson TJ (1994) CLUSTAL W: improving the sensitivity of progressive multiple sequence alignment through sequence weighting, position-specific gap penalties and weight matrix choice. Nucl Acids Res 22:4673–4680

Turk V, Bode W (1991) The cystatins: protein inhibitors of cysteine proteinases. FEBS Lett 285:213–219

Valdés-Rodríguez S, Guerrero-Rangel A, Melgoza-Villagómez C, Chagolla-López A, Delgado-Vargas F, Martínez-Gallardo N, Sánchez-Hernández C, Délano-Frier J (2007) Cloning of a cDNA encoding a cystatin from grain amaranth (*Amaranthus hypochondriacus*) showing a tissue-specific expression that is modified by germination and abiotic stress. Plant Physiol Biochem 45:790–798

van der Vyver C, Schneidereit J, Driscoll S, Turner J, Kunert K, Foyer CH (2003) Oryzacystatin-1 expression in transformed tobacco produces a conditional growth phenotype and enhances chilling tolerance. Plant Biotechnol J 1:101–112

Vorster J, Michaud D, Kiggundu A, Kunert K (2010) Crop damage. Quest 6:30–32

Wang YG, Zhan YN, Wu C, Gong SL, Zhu N, Chen SX, Li HY (2012) Cloning of a cystatin gene from sugar beet M14 that can enhance plant salt tolerance. Plant Sci 191–192:93–99

Wang XM, Li ZG, Yan F, Khalil R, Ren ZX, Yang CW, Yang YW, Deng W (2013) *ZmSKIP*, a homologue of *SKIP* in maize, is

involved in response to abiotic stress in tobacco. Plant Cell Tissue Organ Cult 112:203–216

White RG, Kirkegaard JA (2010) The distribution and abundance of wheat roots in a dense, structured subsoil–implications for water uptake. Plant Cell Environ 33:133–148

Zhang X, Liu S, Takano T (2008) Two cysteine proteinase inhibitors from *Arabidopsis thaliana*, *AtCYSa* and *AtCYSb*, increasing the salt, drought, oxidation and cold tolerance. Plant Mol Biol 68:131–143